Electronic Supplementary Material (ESI) for Nanoscale Advances.
This journal is © The Royal Society of Chemistry 2020

Electronic Supplementary Information

Water dynamics affects thermal transport at the surface of hydrophobic and hydrophilic irradiated nanoparticles

Sebastian Salassi[1], Annalisa Cardellini[2], Pietro Asinari[2], Riccardo Ferrando[1] and Giulia Rossi[1]*
[1]Physics Department, University of Genoa, via Dodecaneso 33, 16146 Genoa, Italy
[2]Department of Energy, Politecnico di Torino, Corso Duca degli Abruzzi 24, 10129 Torino, Italy
[*]rossig@fisica.unige.it

1. Functionalized Au nanoparticles

Each Au nanoparticle (NP) used in this work was generated based on the AuS core structure from Acevedo *et al.,*[1] on our elastic network, as described in the main article. To generate a functionalized NP we used an in house python script (freely available in our on line repository[2]) in order to attach a thiol ligand in each S atom of the core. The obtained configuration, for each ligand type, was minimized in vacuum and then solvated with SPC/E water. The solvated system was minimized and equilibrated for 25 ns in the NPT ensemble with a time step of 2 fs, v-rescale thermostat (T = 300 K and τ_T = 2 ps) and Berendsen barostat (P = 1 bar and τ_P = 1 ps). The output configuration was used as starting point for the equilibrium and non-equilibrium simulations described in the main paper. All the *.itp* and *.gro* files used in this work are available in our online repository.[2]

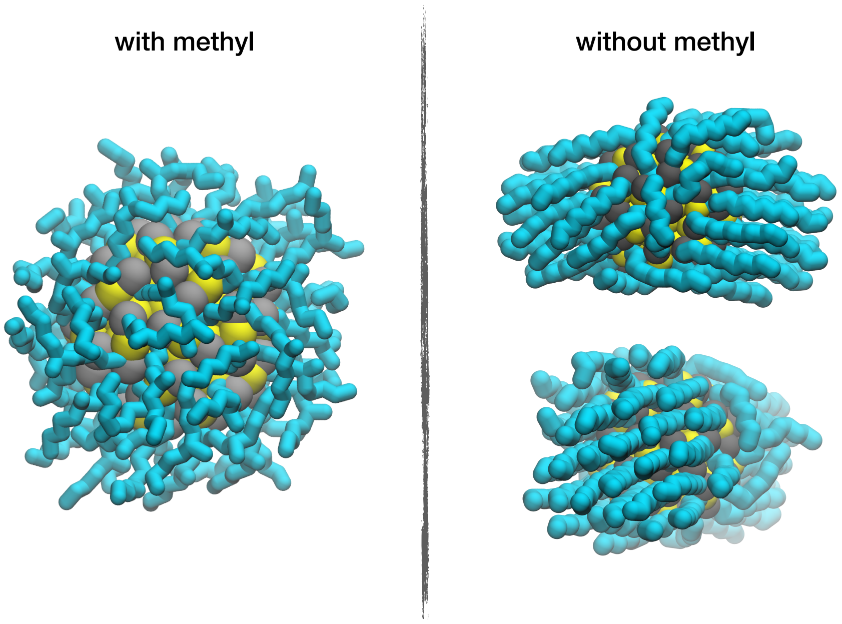

Figure S1. Comparison between the final configuration of a hydrophobic nanoparticle in water: in the left functionalized with the 6-methyl-undecane thiol (MC11) and in the right with the undecane thiol (C11). The addition of the methyl group in the alkyl chains is needed to prevent the ordered packing of the alkane on the NP surface.

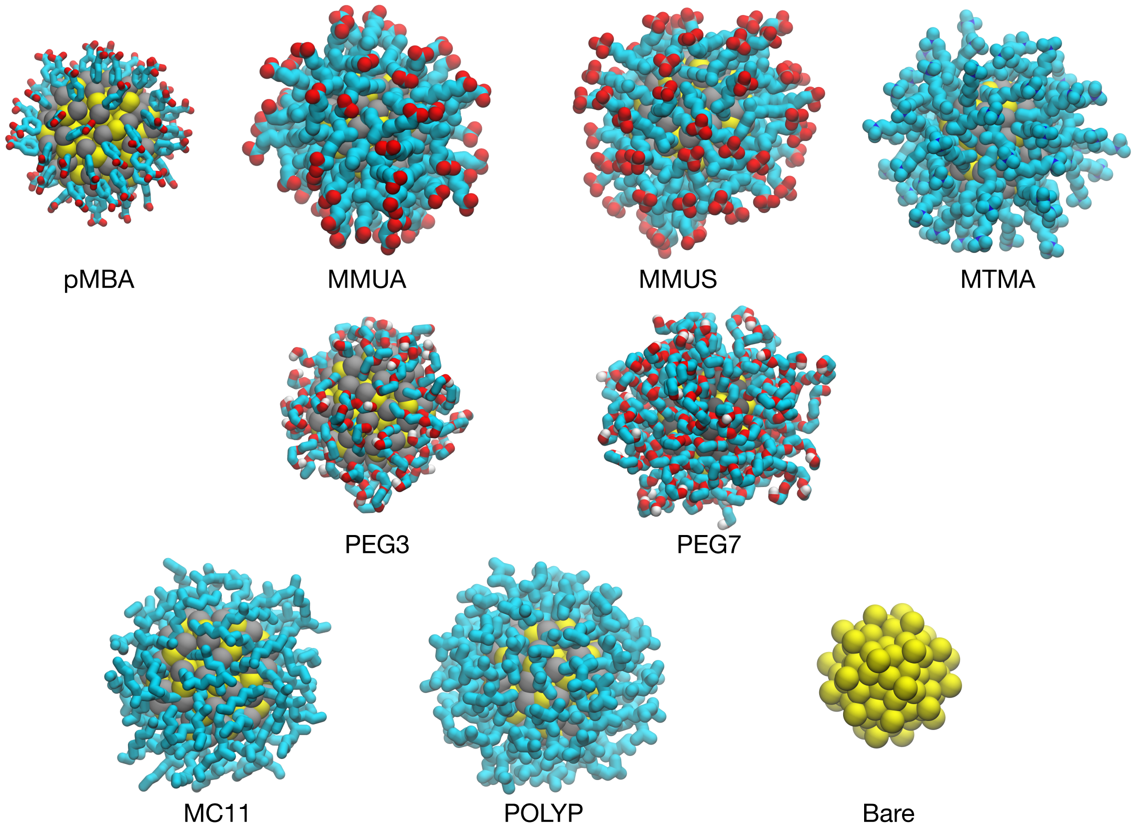

Figure S2. Snapshot assumed by all nanoparticles in the water phase. The Au and S atoms are shown in yellow and grey, respectively. While C in cyan, O in red, N in blue and H in white.

2. Alternative system

We have built an alternative set-up to employ the temperature gradient for non-equilibrium molecular dynamics (NEMD) simulations. We aim at verifying if the constrained cold-water molecules of our main set-up could lead to perturbations such to produce unrealistic temperature profile. The alternative system, shown in the left panel Figure S3, is made by a rigid spherical buckyball of 4894 atoms and a diameter of about 7 nm. The atoms of the buckyball are parametrize like carbon atoms and its density is tuned in such a way that water molecules cannot pass through it. Then, a ligand protected Au NP is placed at the center of the buckyball and the system is solvated with about 39000 SPC/E water molecules. In order to achieve the correct water density, the number of water molecules is tuned accordingly. In Figure S4 it is show the number density of each system part as a function of the distance from the NP center of mass.

For the NEMD simulations the heat source is the Au atoms thermostated at T_{hot} = 380 K and heat sink is the buckyball itself, whose atoms are thermostated at T_{cold}. A comparison of the temperature profile obtained with the two set-ups is shown in the right panel of Figure S3. We choose to perform the NEMD simulations with the alternative system only for the MMUA and MC11 ligand types: these two ligands show two different temperature profiles while they only differ in the functional terminal group (a charged –COO$^-$ for the first ligand and a –CH$_3$ in the second one). As we can see, the temperature profiles are identical for both types.

The alternative NEMD simulations are performed in the NVT ensemble with a time step of 2 fs. The system is pre-equilibrated for 15 ns with v-rescale thermostat (T = 300 K and τ_T = 1 ps) applied separately at Au NP, solvent and buckyball atoms. Then, 65 ns long NEMD simulation was performed with Noose-Hoover thermostat (τ_T = 1 ps), applied at Au atoms (T_{hot} = 380 K) and at buckyball atoms (T_{cold} = 280 K). The temperature profile was obtained discharging the first 15 ns of the trajectory, in order to have the system with the correct temperature gradient.

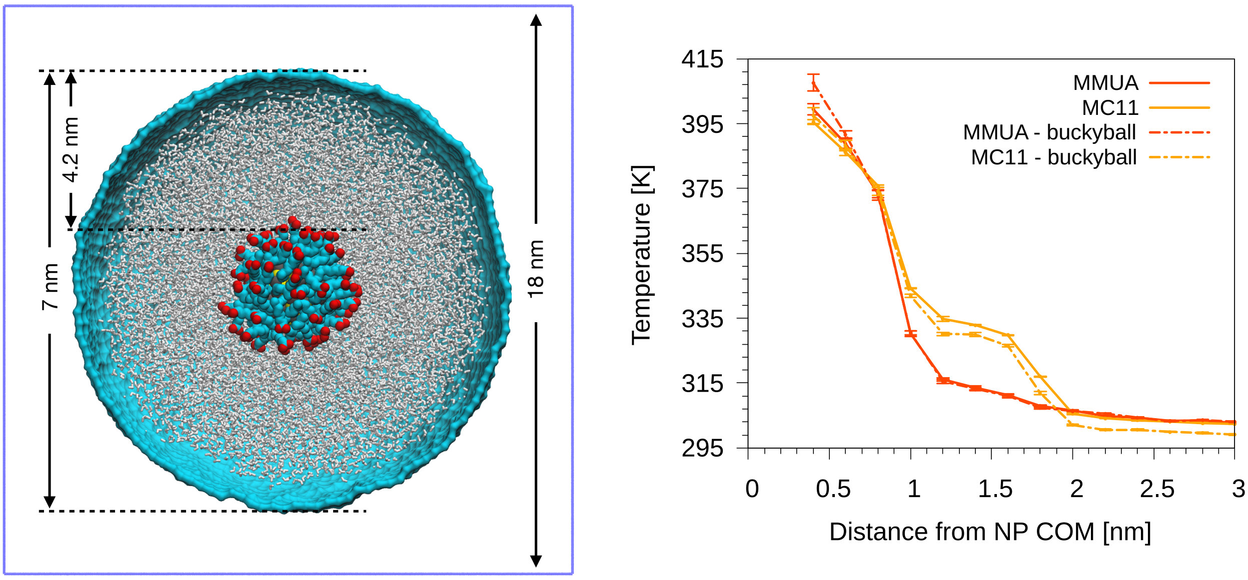

Figure S3. Left: System configuration of the alternative set-up. C atoms in cyan, O in red and water molecules as white sticks. Right: Temperature profiles of MMUA and MC11 ligand types for both set-ups as a function of the distance from the nanoparticle center of mass.

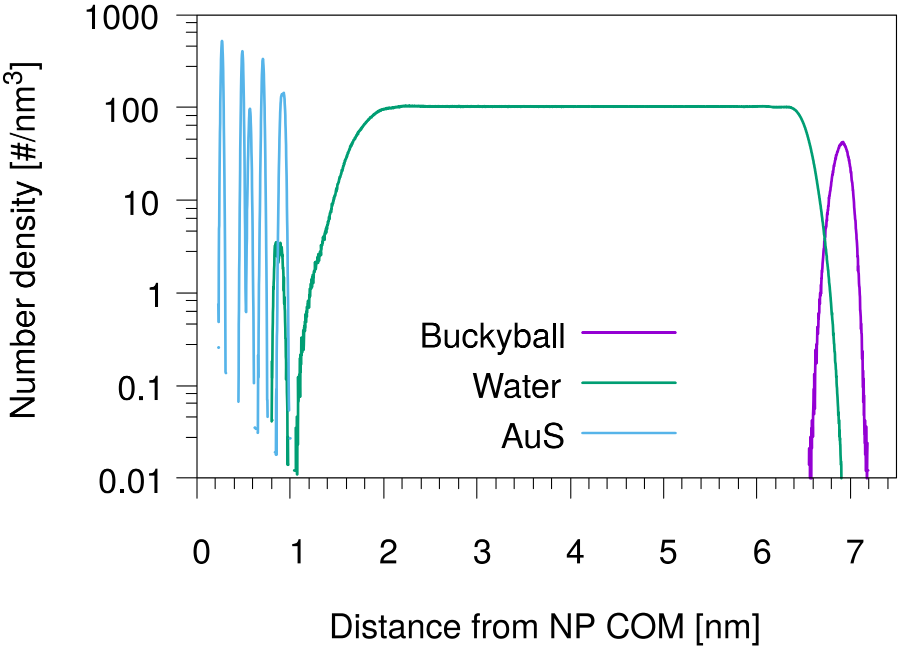

Figure S4. Number density of each system part (excluded the functionalizing ligands) of the alternative set-up as a function of the distance from the nanoparticle center of mass.

Ligand name	**ΔT_{AuL} [K]**	**ΔT_{LW} [K]**	**R**	**δ [nm]**	**ε [kJ mol^{-1}]**	**$\varepsilon/(k_B T_{\mathrm{LW}} N_A)$**	**$r_{\mathrm{L}} - r_{\mathrm{W}}$ [nm]**
MC11	31.6 ± 0.4	24.3 ± 0.3	0.565 ± 0.009	0.34 ± 0.01	–3.7 ± 0.1	–1.48 ± 0.06	1.5 – 1.7
PEG7	41.1 ± 0.8	5.3 ± 0.3	0.89 ± 0.02	0.35 ± 0.01	–4.6 ± 0.2	–1.80 ± 0.07	1.7 – 2.1
MMUA	42.4 ± 0.8	5.0 ± 0.3	0.89 ± 0.02	0.342 ± 0.009	–4.3 ± 0.1	–1.69 ± 0.04	1.6 – 2.0
PEG3	41.5 ± 0.7	4.1 ± 0.3	0.91 ± 0.02	0.37 ± 0.02	–4.3 ± 0.2	–1.68 ± 0.08	1.4 – 1.6
pMBA	39.8 ± 0.7	2.1 ± 0.4	0.95 ± 0.02	0.385 ± 0.009	–4.7 ± 0.1	–1.83 ± 0.04	1.3 – 1.5
bare	48.7 ± 0.7	-	1.00 ± 0.02	0.463 ± 0.006	–12.0 ± 0.2	–4.41 ± 0.06	-
POLYP	30.6 ± 0.7	21.4 ± 0.3	0.59 ± 0.02	0.36 ± 0.02	-3.8 ± 0.2	-1.48 ± 0.08	1.6 – 2.0
MTMA	40.6 ± 0.07	8.2 ± 0.3	0.83 ± 0.02	0.328 ± 0.007	-3.86 ± 0.09	-1.52 ± 0.03	1.6 – 2.1
MMUS	42.5 ± 0.7	5.8 ± 0.3	0.88 ± 0.02	0.37 ± 0.01	-4.3 ± 0.1	-1.69 ± 0.04	1.6 – 2.0

Table S1. Values of the temperature drops at Au–ligand and ligand–water interfaces, the dimensionless parameter R (see Equation 1 of the main paper), the characteristic water confinement length (δ) and energy (ε), normalized-ε, and the spatial extension of the ligand–water interface ($r_{\mathrm{L}} - r_{\mathrm{W}}$).

Ligand name	**R**	**D_{int} [10^{-5} cm^2 s^{-1}]**	**D_{bulk} [10^{-5} cm^2 s^{-1}]**	**τ_r [ps]**
MC11	0.565 ± 0.009	1.72 ± 0.06	2.9 ± 0.2	0.7
PEG7	0.89 ± 0.02	1.22 ± 0.02	2.72 ± 0.05	15
MMUA	0.89 ± 0.02	1.25 ± 0.04	2.70 ± 0.03	25
PEG3	0.91 ± 0.02	1.42 ± 0.08	2.81 ± 0.03	16
pMBA	0.95 ± 0.02	0.74 ± 0.03	2.93 ± 0.06	42
bare	1.00 ± 0.02	0.88 ± 0.03	2.92 ± 0.06	40

Table S2 Value of the R parameter (see Equation 1 of the main paper), the water self-diffusion coefficient at ligand-water interface (D_{int}) and in the bulk (D_{bulk}) and of the water characteristic residence time (τ_r) for each type of ligand.

3. Fit of the normalized-ε and δ.

The hyperbolic fit of the plots in Figure 3B and 3C in the main text is performed with the *gnuplot* package taking into account the statistical errors of both *x* and *y* axes. Each dataset *f(R)*, which could be $\varepsilon(R)$ or $\delta(R)$, is first linearized, fixing the asymptote parallel to the *y*-axis to $R = 1$, and then fitted against a linear relationship *h(R)*:

$$h(R) = f(R)(R-1) = aR + b$$

where: *f(R)* is the hyperbolic function plotted in Figure 3B and 3C. The values of the fitting parameters for the normalized-ε and δ are shown in Table S2.

	a	*b*
normalized-ε	-1.44 ± 0.05	1.46 ± 0.04
δ	-0.339 ± 0.004 nm	0.337 ± 0.005 nm

Table S3. Fitting parameters for normalized-ε and δ.

4. Error estimation to ε and δ.

The error estimation to ε and δ was derived following the statistical error propagation theory. Following the work of Chiavazzo *et al.*[3] ε and δ are defined by the following equations:

$$\varepsilon = \frac{1}{S}\left(\sum_i \varepsilon_i s_i\right) = \frac{\sum_i \varepsilon_i s_i}{\sum_i s_i}, \qquad \delta = \frac{\sum_i \delta_i s_i}{\sum_i s_i}$$

Where *S* is the total solvent accessible surface area (SASA) defined as:

$$S = \sum_i s_i\,, \qquad \sigma_S^2 = \sum_i \sigma_{s_i}^2$$

and s_i is the SASA for the *i*th atom of the NP.

Then, the error propagation of ε reads as:

$$\frac{\sigma_\varepsilon^2}{\varepsilon^2} = \frac{\sum_i \sigma_{s_i}^2}{S^2} + \frac{\sum_i \varepsilon_i^2\,\sigma_{s_i}^2}{\left(\sum_i \varepsilon_i s_i\right)^2} = \frac{1}{S^2}\left(\sum_i \sigma_{s_i}^2 + \frac{\sum_i \varepsilon_i^2\,\sigma_{s_i}^2}{\varepsilon^2}\right)$$

$$\sigma_\varepsilon^2 = \frac{1}{S^2}\left(\varepsilon^2 \sum_i \sigma_{s_i}^2 + \sum_i \varepsilon_i^2\,\sigma_{s_i}^2\right)$$

In the same way for δ, we have:

$$\sigma_\delta^2 = \frac{1}{S^2}\left(\delta^2 \sum_i \sigma_{s_i}^2 + \sum_i \delta_i^2\,\sigma_{s_i}^2\right)$$

5. Vibrational density of states

The vibrational density of states (vDOS) as a function of the frequency, $S(\nu)$, are calculated through the double precision version of the Gromacs *gmx dos* tool,[4] in which the vDOS spectrum is calculated by the Fourier transform of the mass-weighted velocity autocorrelation function.[5] $S(\nu)$ is define such that the integral over ν is the total degrees of freedom.[5] To compute the vDOS a 20 ps long trajectory with a saving frequency of 1 fs is used (for both positions and velocities). This simulation has been performed in double precision and in the microcanonical ensemble (NVE) using the velocity-verlet integrator with a time step of 0.1 fs and a cut-off for the short-range neighbor list of 1.3 nm (to ensure a better energy conservation).

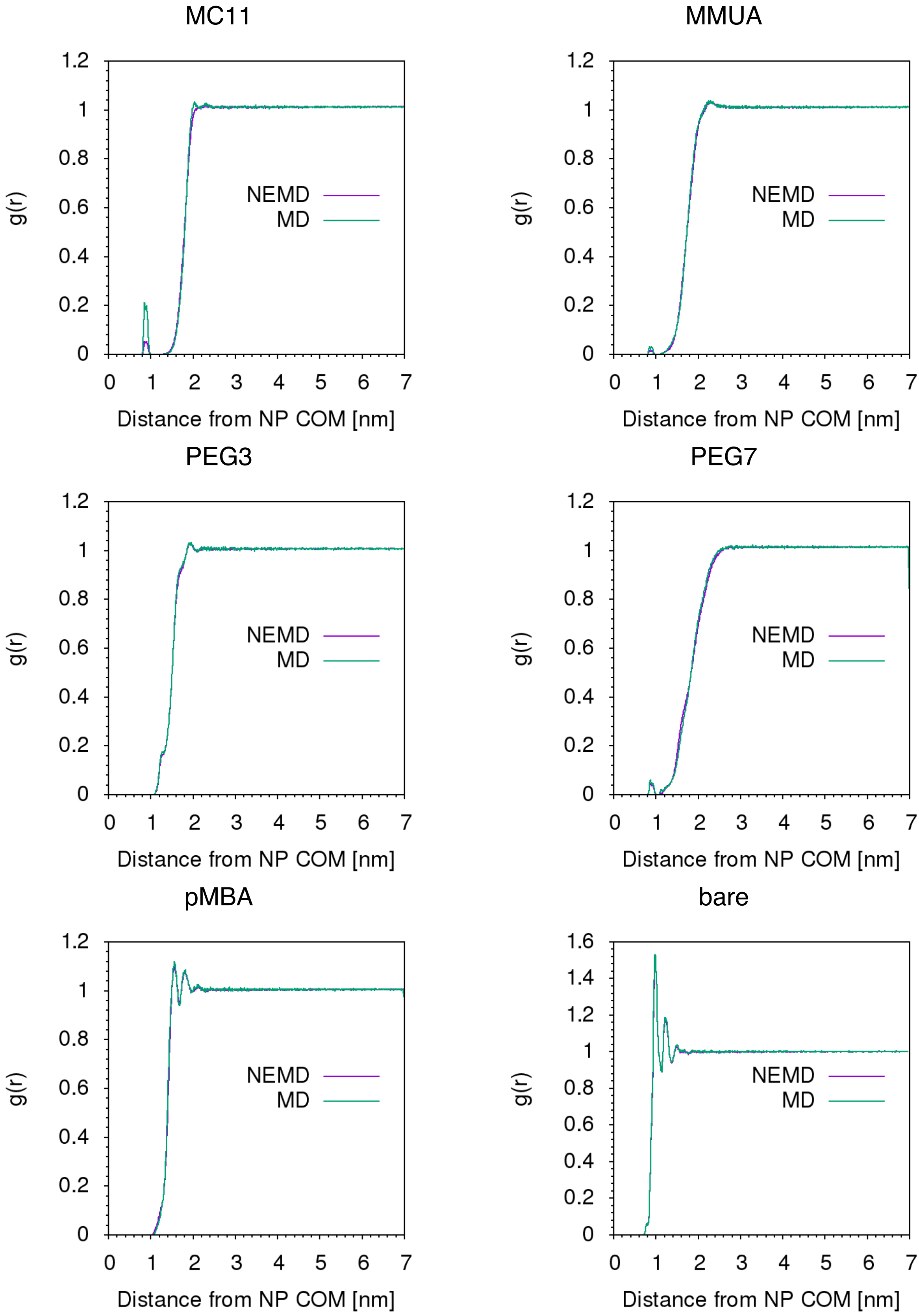

Figure S5. Plot of the water radial distribution function, *g*(*r*), in a comparison between equilibrium and non-equilibrium MD simulations, for each type of NP.

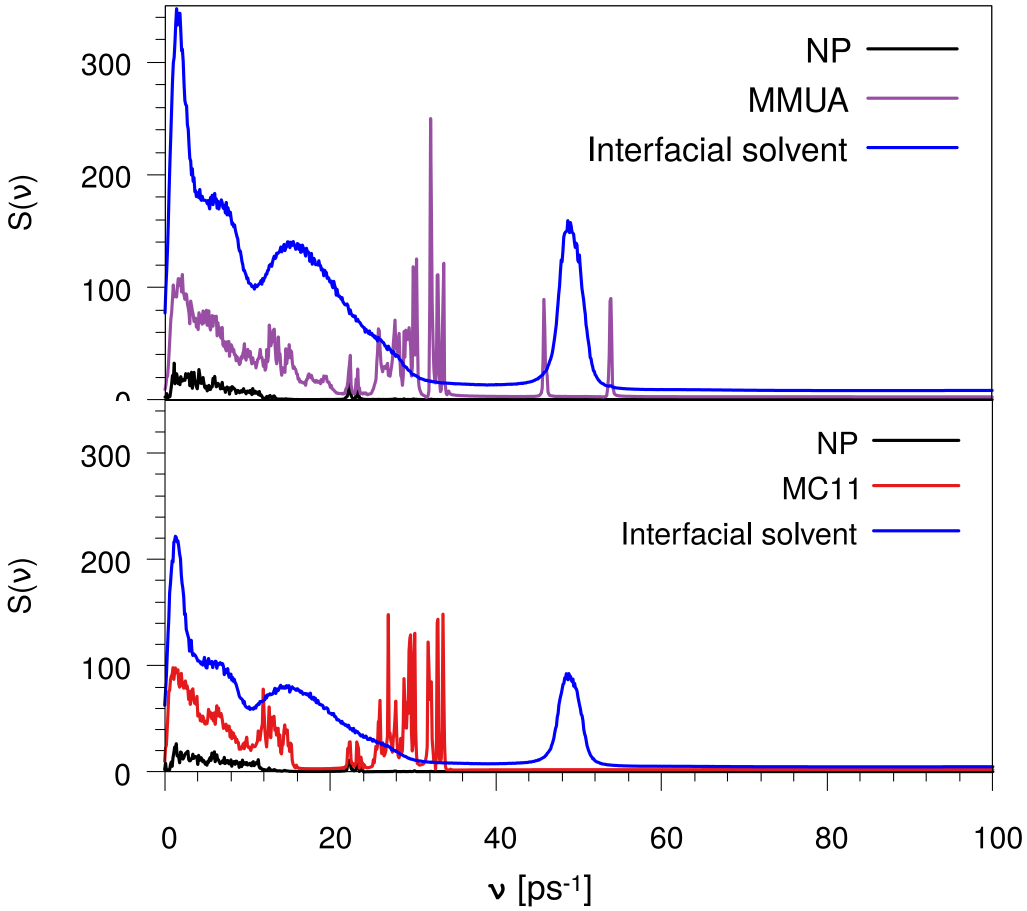

Figure S6. Plot of vDOS for core atoms (black lines), ligand atoms (red and purple lines) and water molecules at the interface (blue lines) for the MC11 (top panel) and MMUA (bottom panel) NPs. The two spectra for the interfacial solvent have the same shape but different normalization because of the different number of water molecules at interfaces: less for the MC11 than that for the MMUA.

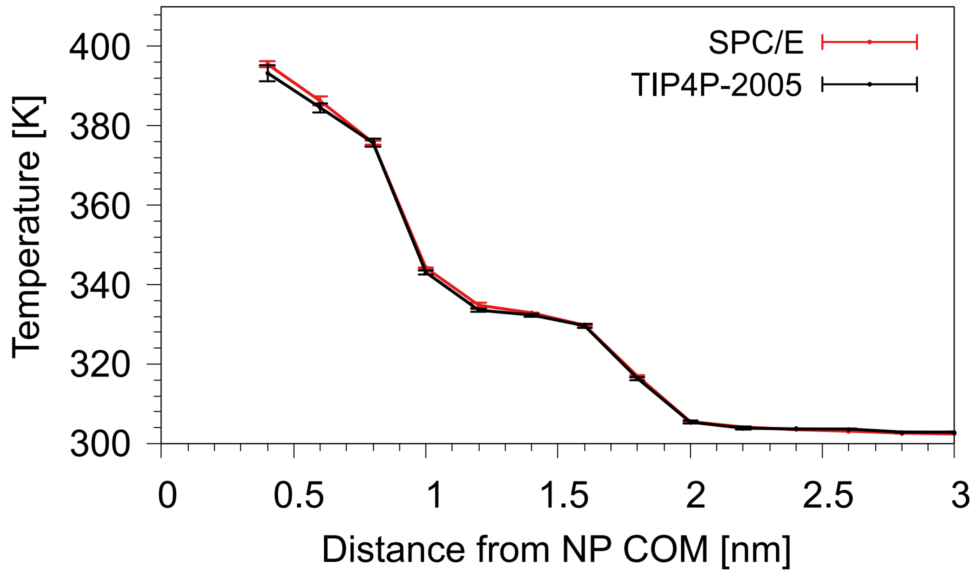

Figure S7. Comparison between the temperature profile of the MC11 as obtained with the SPC/E and with the TIP4P-2005 water model, with identical simulation conditions.

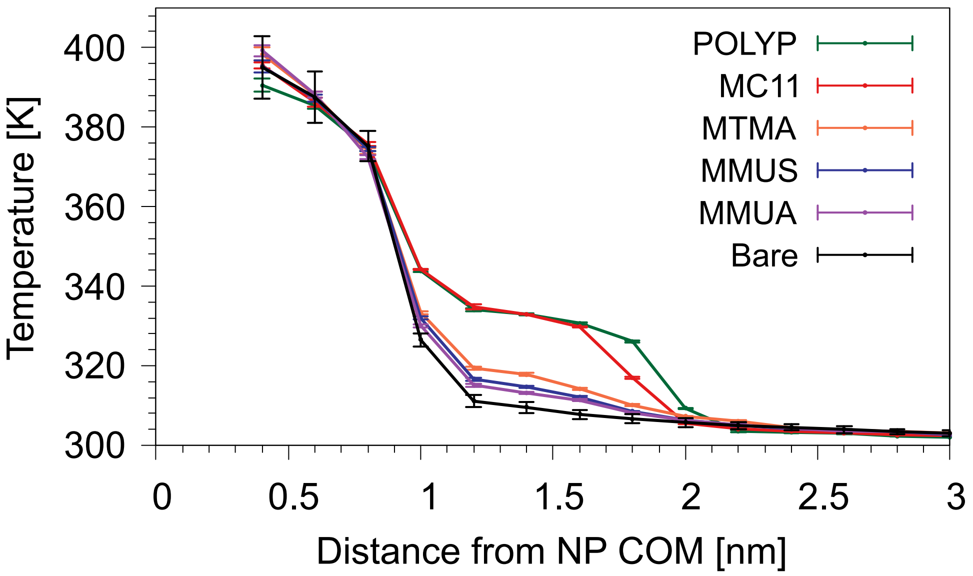

Figure S8. Temperature profiles for the ligands used for validation (POLYP, MMUS, MTMA) compared to those used for model development.

References

1 O. Lopez-Acevedo, J. Akola, R. L. Whetten, H. Grönbeck and H. Häkkinen, *J. Phys. Chem. C*, 2009, **113**, 5035–5038.

2 https://bitbucket.org/biomembnp/biomembnp, BioMembNP repository, https://bitbucket.org/biomembnp/biomembnp.

3 E. Chiavazzo, M. Fasano, P. Asinari and P. Decuzzi, *Nat. Commun.*, 2014, **5**, 1–11.

4 T. A. Pascal, S. T. Lin and W. A. Goddard, *Phys. Chem. Chem. Phys.*, 2011, **13**, 169–181.

5 S. T. Lin, M. Blanco and W. A. Goddard, *J. Chem. Phys.*, 2003, **119**, 11792–11805.